water contents near the liquid limit. These samples have enough strength to allow extrusion and trimming and have a relatively small preconsolidation pressure (σ'_p < 50kPa).

After a JPC tube was selected, the end seals were removed. The tube was fixed on a horizontal circular vise and cut at 2 locations to the desired lengths using a rotating tube cutter. The tube cutter was turned slowly while applying gentle pressure such that there was no visual evidence of damage. A wire saw was passed through the 2 cuts and the clay was extruded. The soil was pushed upwards in the same direction of movement during sampling. Following extrusion, the clay was trimmed with a wire-saw. On average, the specimen diameter was 33.7mm (31.1-36.0mm) and the specimen height was 71.9mm (65.3-75.6mm), resulting in an average H/D ratio of 2.1. Vertical filter paper side drains were attached to specimens to speed consolidation. For each specimen, a latex membrane with a thickness of 0.30mm was used. The specimen was then carefully mounted in the cyclic triaxial apparatus, back-pressure saturated (B coefficient > 0.97) and consolidated to an equal all-around pressure of at least twice the preconsolidation pressure. Preconsolidation pressure was estimated from:

1. End-of-primary (EOP) e – log σ'_v curves obtained from incremental loading oedometer tests. Constructions used were the Casagrande, Oikawa (1987), and work per unit volume methods (Becker et al., 1987).
2. An estimation of σ'_{vo} from bulk density measurements from specimen weight and dimensions and an assumed OCR ~ 2 at shallow depth (Rafalovich and Chaney, 1990).
3. CPT results (Lunne and Andersen, 2007; Mesri, 2001).

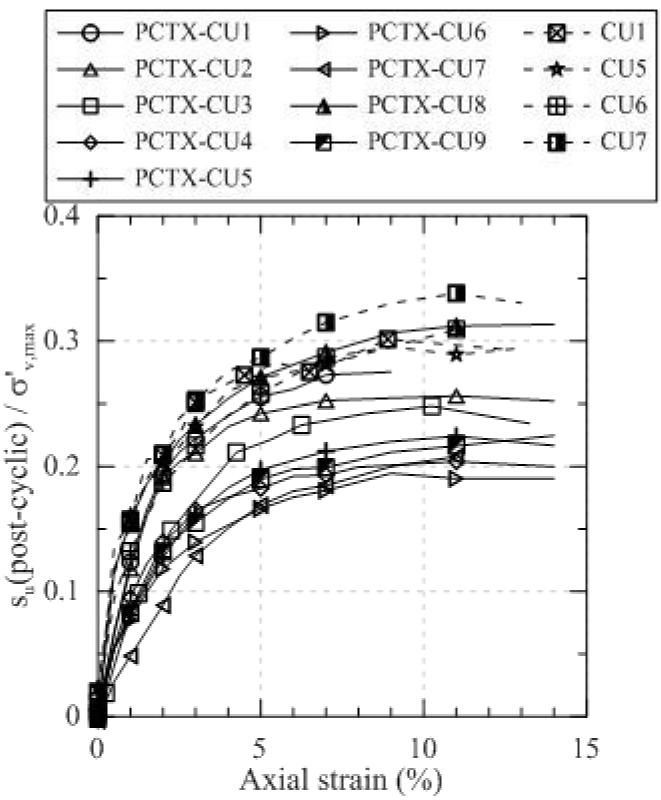

Figure 1: Stress-strain plots for 9 post-cyclic undrained compression tests and 4 typical undrained compression tests

Testing program

After the Gulf of Mexico clay specimens were consolidated to the virgin compression zone to an equal all-around pressure $\sigma'_{v,max}$, an overconsolidation was induced by reducing the cell pressure and allowing them to rebound to a smaller effective stress. For OCR = 1 tests, the latter step was omitted. Once the desired OCR was achieved, the specimens were subjected to 300 sinusoidal cycles at a frequency of 0.5Hz. The cyclic single strain amplitudes (SSA) and the general testing program are shown in .

Following the cyclic event, the cyclically induced excess PWP, Δu(cyclic), was allowed to equalize without drainage and the specimens were tested in undrained compression at an average strain rate of 0.40 %/hr (0.30 – 0.66 %/hr).

RESULTS AND DISCUSSIONS

The results of the post-cyclic undrained compression tests are shown in Table 2 and Figure 1. Also shown in Figure 2 are the normalized stress-strain plots of four monotonic undrained compression tests ran without prior cycling (OCR=1, I_p = 40-50%, w_0=66-94%) (CU1, CU5, CU6, CU7). There was no noticeable change in the strain at failure, which averaged about 9% (8-11%) for the post-cyclic undrained compression tests. For the undrained compression carried out without prior cycling, the strain at failure was about 8%.

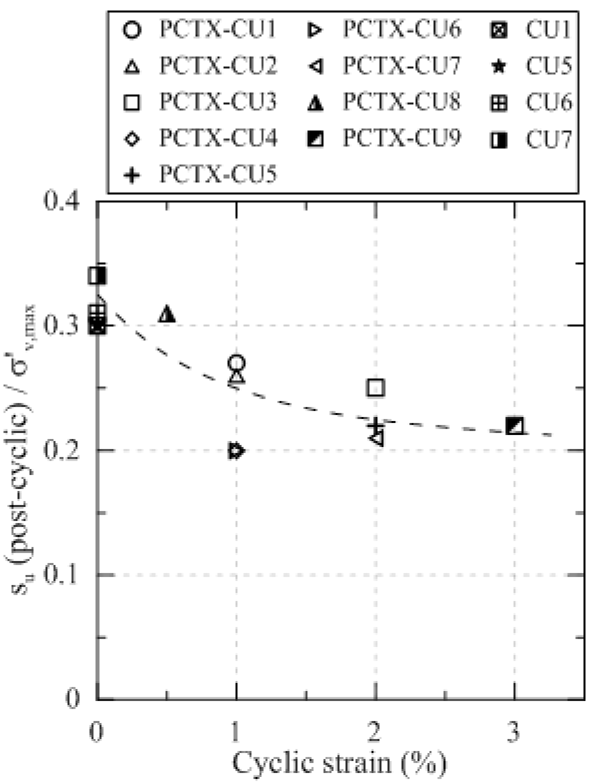

Figure 2: Normalized post-cyclic undrained shear strength vs. cyclic strain for the 9 post-cyclic undrained compression tests

As shown in Figure 2, the available post-cyclic undrained shear strength normalized by the maximum effective stress experienced by a specimen, s_u(post-cyclic)/$\sigma'_{v,max}$, decreases with cyclic strain amplitude. The larger the applied cyclic strain, the more significant is the disturbance to the clay fabric and therefore, the smaller the post-cyclic undrained shear strength. A cyclic strain amplitude of 0.5% resulted in a s_u(post-cyclic)/$\sigma'_{v,max}$ of 0.31, implying that γ_c = 0.5% is slightly higher than the threshold shear strain for strength reduction (e.g. Vucetic, 1994). For 300 cycles at 0.5Hz at 0.5-3% single strain amplitude, s_u(post-cyclic)/$\sigma'_{v,max}$ of Gulf of Mexico clay ranges from 0.20 to 0.31, representing a 5 to 35% decrease in shear strength from monotonic tests. Erken and Ülker (2008) and Li et al. (2011) showed that cycling of clays decreases the undrained shear strength by 20% and 30% respectively.

Table 1: Summary of the testing program

Test	Sampling depth (m)	w_0 (%)	Diameter (mm)	$\sigma'_{cons.,1}$[a] (kPa)	$\sigma'_{cons.,2}$[b] (kPa)	OCR achieved	SSA[c] (%)	Δu(cyclic)/ $\sigma'_{v,max}$[d]
PCTX-CU1	5.1	83	36.0	181	181	1.0	1	0.27
PCTX-CU2	5.2	82	35.5	229	229	1.0	1	0.23
PCTX-CU3	5.3	81	31.1	248	248	1.0	2	0.33
PCTX-CU4	5.6	83	34.4	199	104	1.9	1	0.14
PCTX-CU5	5.7	83	32.4	204	105	1.9	2	0.17
PCTX-CU6	5.4	80	35.7	153	45	3.4	1	0.00
PCTX-CU7	5.5	83	34.7	159	53	3.0	2	0.03
PCTX-CU8	3.1	91	31.6	204	205	1.0	0.5	0.10
PCTX-CU9	3.2	92	32.1	225	222	1.0	3	0.40

[a]Effective equal all-around pressure during first stage of consolidation
[b]Effective equal all-around pressure prior to cycling
[c]Single strain amplitude (axial) during cycling portion of test
[d]Cyclically induced excess PWP normalized by the maximum effective stress

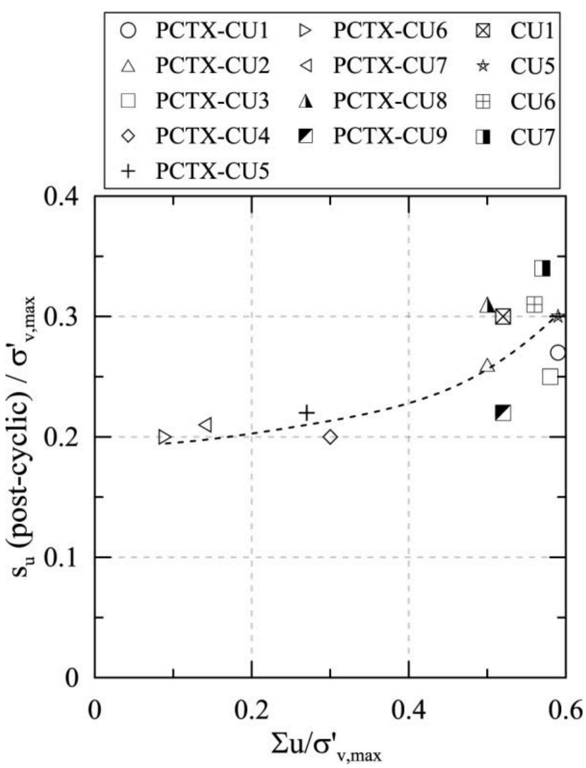

Figure 3: Normalized post-cyclic undrained shear strength vs. normalized total shear-induced excess PWP for the 9 post-cyclic undrained compression tests

Figure 3 shows the plot of s_u(post-cyclic)/$\sigma'_{v,max}$ vs. $\Sigma[\Delta u]/\sigma'_{v,max}$, where the latter is the sum of PWP induced during the cyclic and post-cyclic monotonic stages normalized by $\sigma'_{v,max}$. The scatter in the data is relatively large and no relationship between s_u(post-cyclic)/$\sigma'_{v,max}$ vs. $\Sigma[\Delta u]/\sigma'_{v,max}$ can be effectively drawn. However, when $\Sigma[\Delta u]/\sigma'_{v,max}$ was plotted vs. OCR as shown in Figure 4, a definite trend can be observed, independent of cyclic strain. This suggests that the potential for excess PWP generation is heavily dependent on OCR, irrespective of how failure is brought about (cyclic and/or monotonic).

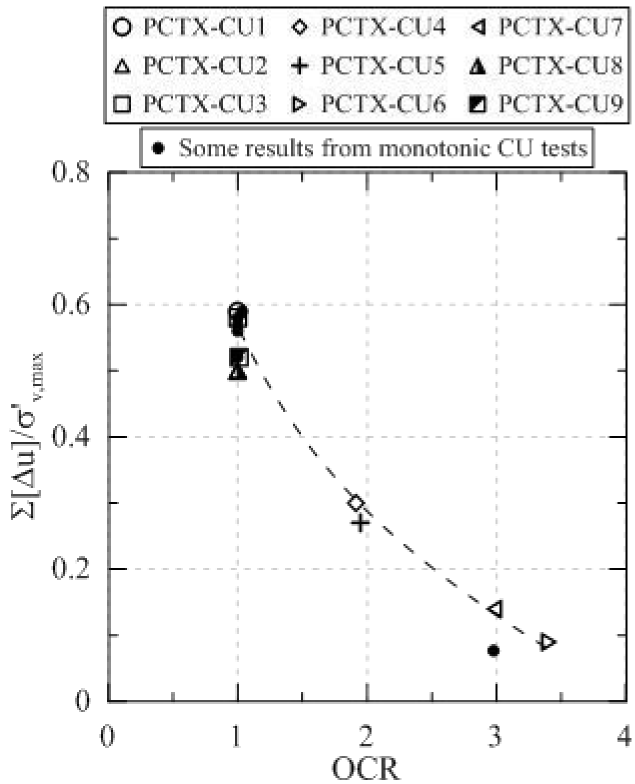

Figure 4: Normalized total shear-induced PWP vs. pre-cyclic OCR

Another way to look at post-cyclic strength loss is to relate it to shear modulus degradation suffered by the clay during cycling (Idriss et al., 1978). Figure 5 shows the relationship between s_u(post-cyclic)/$\sigma'_{v,max}$ and degradation parameter “t”, where $G_N/G_1 = N^{-t}$ (G_1 is the shear modulus at cycle N=1). G_N was calculated as the slope of a line connecting the apexes of the stress-strain loops during cycling. The higher the degradation parameter “t”, the more damage the clay fabric has suffered and more significant is the reduction in undrained shear strength.

Figure 6 and Figure 7 show the relationship between the secant E(post-cyclic)/$\sigma'_{v,max}$ calculated for axial strains of 0.5% and 1%, respectively, during post-cyclic undrained monotonic compression and degradation parameter “t”. Although there is significant scatter, the data illustrate that the higher the degradation parameter “t”, the smaller the value E (post-cyclic)/$\sigma'_{v,max}$. That is, the more disrupted the clay fabric gets during cycling, less stiff the subsequent stress-strain undrained monotonic response.

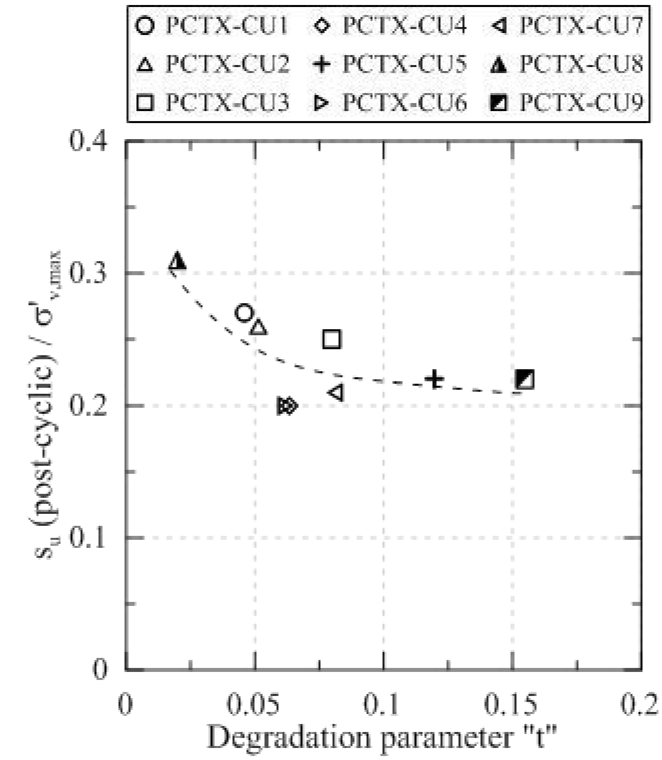

Figure 5: Normalized post-cyclic undrained shear strength vs. degradation parameter "t"

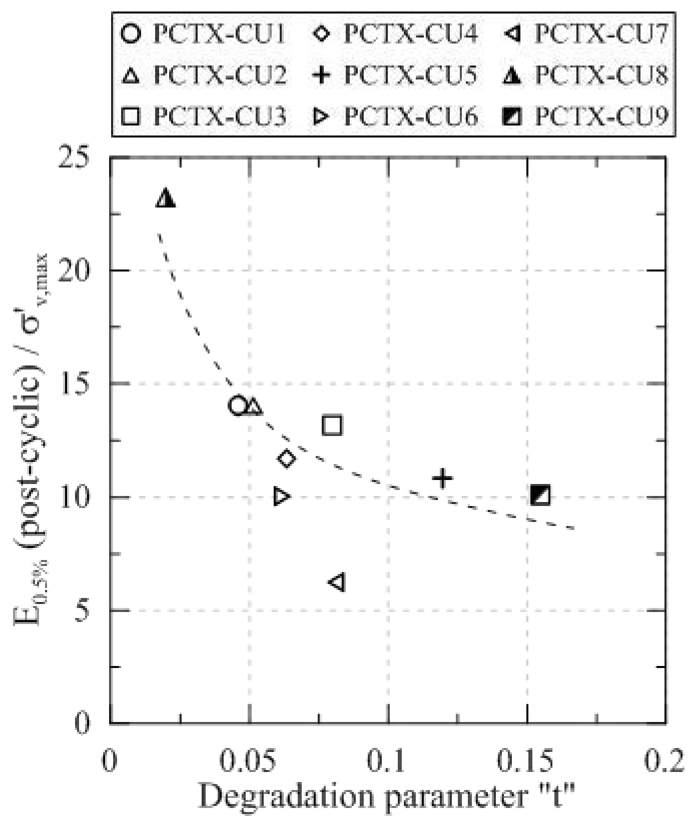

Figure 6: Secant E (post-cyclic)/$\sigma'_{v,max}$ for axial strain = 0.5% vs. degradation parameter "t"

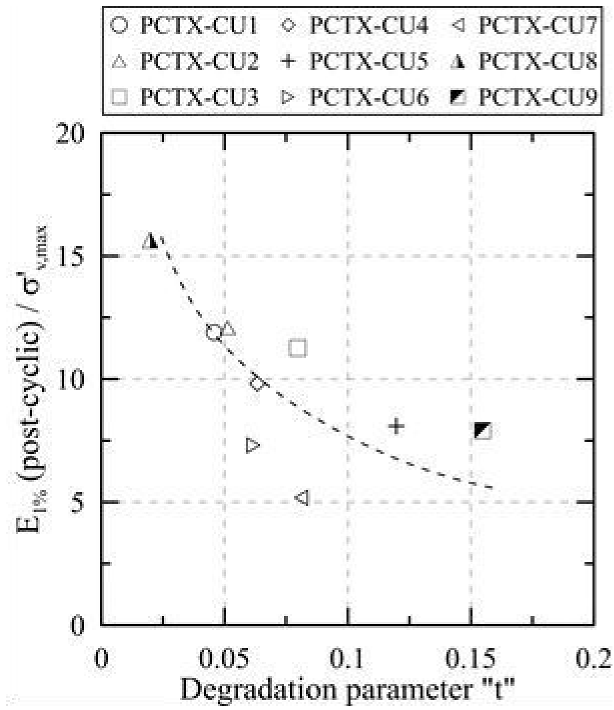

Figure 7: Secant E (post-cyclic)/σ'$_{v,max}$ for axial strain = 1% vs. degradation parameter "t"

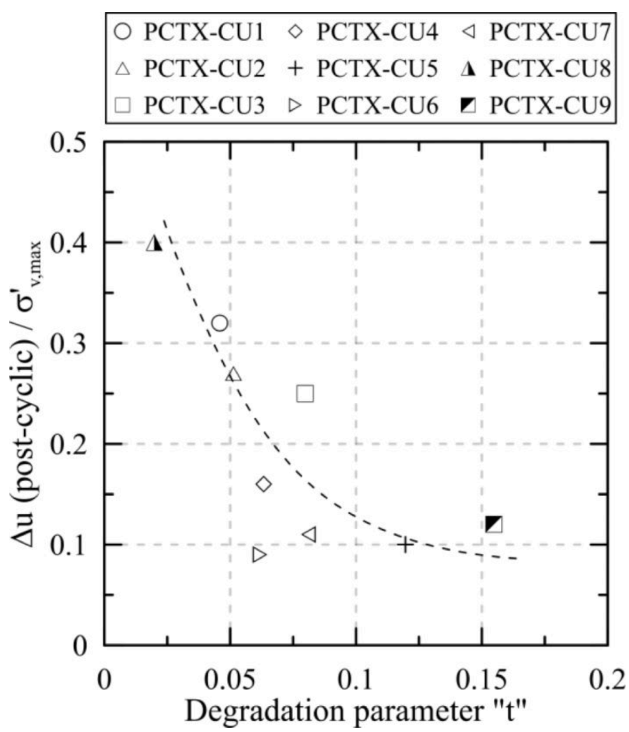

Figure 8: Normalized excess PWP induced during compression vs. degradation parameter "t"

Figure 8 shows that relationship between degradation parameter "t" and Δu(post-cyclic)/σ'$_{v,max}$. As the degradation parameter "t" is indicative of fabric damage and shear strength loss (for a given number of cycles), the degradation parameter “t” also is related to the excess PWP generated during post-cyclic undrained monotonic shearing. The more damaged the clay fabric, the lesser the tendency to contract (during post-cyclic monotonic loading) and the smaller should be Δu(post-cyclic)/$\sigma'_{v,max}$.

Figure 9 shows the stress paths for all post-cyclic monotonic compression tests (PCTX-CU1 – PCTX-CU9) and the typical undrained compression tests (CU1, CU5, CU6 and CU7). Included are some drained fully-softened failure envelopes suggested in the literature (Murali, 2011; Silva et al., 2000; Chaney and Fang, 1986;, Esrig et al, 1975; Mesri and Shahien, 2003;, Stark and Hussain, 2013). It can be seen that all post-cyclic tests showed a dilative behavior (except PCTX-CU8) but end on the same failure envelope. PCTX-CU8 showed a contractive response, implying that a 0.5% single strain amplitude was not enough to damage the fabric. The failure envelope represents large strain behavior, which is controlled by mineralogy and not influenced by factors such as the original fabric and aging. Hence, the same failure envelope is applicable for the Gulf of Mexico clay brought to failure monotonically or through a combination of cyclic and monotonic straining.

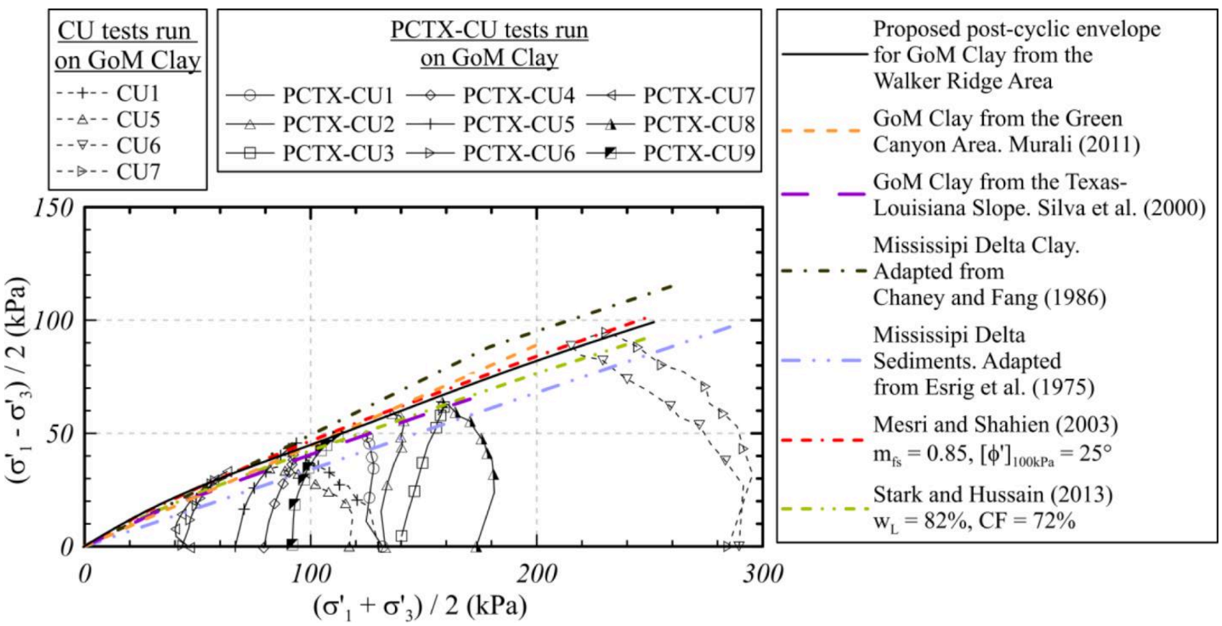

Figure 9: The 9 post-cyclic compression tests and the 4 undrained compression tests plotted in a stress-path space. Included are some failure envelopes reported in the literature.

CONCLUSIONS

Based on a series of strain-controlled cyclic triaxial tests on soft normally consolidated to lightly overconsolidated Gulf of Mexico clay, the following conclusions can be drawn:

1. A cyclic event does not influence the strain at which a soft clay fails in undrained compression.
2. The higher the cyclic strain amplitude, the more damage to the soil fabric and the lower the s_u(post-cyclic)/$\sigma'_{v,max}$. The strength reduction reported in this paper was of the order of 25% corresponding to a range of single strain amplitude = 0.5-3%.
3. Degradation parameter “t” is indicative of the fabric damage brought about by cycling and is closely related to the slope of the post-cyclic stress-strain curve and the excess PWP generated during undrained compression.

4. The same drained, fully-softened failure envelope applies to intact soft clays and pre-cycled soft clays with the same mineralogical composition.
5. The threshold cyclic strain for strength reduction of Gulf of Mexico clay is around 0.5%.

Table 2: Summary of test results

Test	Δu(post-cyclic)/$\sigma'_{v,max}$[a]	$\Sigma[\Delta u]/\sigma'_{v,max}$[b]	s_u (post-cyclic)/$\sigma'_{v,max}$	Degradation parameter "t"	E (post-cyclic) /$\sigma'_{v,max}$ at strain=0.5%[c]	E (post-cyclic) /$\sigma'_{v,max}$ at strain=1%[d]
PCTX-CU1	0.32	0.59	0.27	0.046	14	12
PCTX-CU2	0.27	0.50	0.26	0.051	14	12
PCTX-CU3	0.25	0.58	0.25	0.080	13	11
PCTX-CU4	0.16	0.30	0.20	0.063	12	10
PCTX-CU5	0.10	0.27	0.22	0.120	11	8
PCTX-CU6	0.09	0.09	0.20	0.062	10	7
PCTX-CU7	0.11	0.14	0.21	0.081	6	5
PCTX-CU8	0.40	0.50	0.31	0.020	23	16
PCTX-CU9	0.12	0.52	0.22	0.155	10	8

[a]Normalized maximum excess PWP generated during monotonic compression
[b]Normalized sum of excess PWP during cyclic event and during monotonic compression
[c]Secant modulus calculated at an axial strain of 0.5% during monotonic compression normalized by $\sigma'_{v,max}$
[d]Secant modulus calculated at an axial strain of 1% during monotonic compression normalized by $\sigma'_{v,max}$

REFERENCES

Andersen, K. H. and Høeg, K. (1991). Deformations of soils and displacements of structures subjected to combined static and cyclic loads. In Proceedings of the 10th European Conference on Soil Mechanics and Foundation Engineering, Vol 4., 1147 – 1158.

Andresen, A. (1981). Exploration, sampling and in situ testing of soft clay. Soft clay engineering (Eds. E. W. Brand and R. P. Brenner). Developments in Geotechnical Engineering, No. 20, Elsevier Science Publishers, Amsterdam, The Netherlands, 241–308.

Becker, D. E., Crooks, J. H. A., Been, K. and Jefferies, M. G. (1987). Work as a criterion for determining in situ and yield stresses in clays. Canadian Geotechnical Journal, Vol. 24(4), 549-564. DOI 10.1139/t87-070

Chaney, R. C. and Fang, H. Y. (1986) Static and Dynamic Properties of Marine Sediments: A State of the Art. Marine Geotechnology and Nearshore/Offshore Structures. ASTM STP 923, R. (C. Chaney and H. Y. Fang, Eds.), American Society for Testing and Materials, Philadelphia, 74-111.

Dobry, R. and Vucetic, M. (1987). State-of-the-art report: Dynamic properties and response of soft clay deposits. Proceedings of the International Symposium on Geotechnical Engineering of Soft Soils, Eds, M. J. Mendoza and L. Montanez, Sociedad Mexicana de Mecanica de Suelos, Mexico City, Vol. 2, 51 – 87.

Erken, A. and Ülker, M.B.C. (2008). The Post-Cyclic Shear Strength of Fine Grained Soils. The 14th World Conference on Earthquake Engineering, Beijing, China.

Esrig, M. I., Ladd, R. S., and Bea, R. G. (1975). Material Properties of Submarine Mississippi Delta Sediments Under Simulated Wave Loadings. Offshore Technology Conference. Paper Number 2188. DOI:10.4043/2188-MS

Idriss, I. M., Dobry, R. and Singh, R. D. (1978). Non-linear behavior of soft clays during cyclic loading. Journal of the Geotechnical Engineering Division, ASCE, GT12, 1427-1447.
Jeanjean, P., Spikula, D. and Young, A. (2012). Technical Vetting of Free-Fall Cone Penetrometer. Proceedings of the Offshore Site Investigation and Geotechnics: Integrated Technologies - Present and Future, Society for Underwater, U.K., 179–186.
Li, L. L., Dan, H. B. and Wang, L.Z. (2011) Undrained behavior of natural marine clay under cyclic loading. Ocean Engineering, Vol. 38, 1792–1805. DOI: 10.1016/j.oceaneng.2011.09.004
Lunne, T. and Andersen, K. H. (2007) Soft clay shear strength parameters for deepwater geotechnical design. Proceedings of the 6th International Offshore Site Investigation and Geotechnics Conference: Confronting New Challenges and Sharing Knowledge, U.K., 151-176.
Makdisi, F. I. and Seed, H. B. (1978). Simplified procedure for estimating dam and embankment earthquake-induced deformation. Journal of Geotechnical Engineering Division, ASCE, Vol. 104 (GT7), 849 – 867.
Mesri, G. (2001). Undrained shear strength of soft clays from push cone penetration test. Géotechnique, Vol. 51 (2), 167–168. DOI:10.1680/geot.2001.51.2.167.
Mesri, G. and Shahien, M. (2003). Residual Shear Strength Mobilized in First-Time Slope Failures. Journal of Geotechnical and Geoenvironmental Engineering, Vol. 129 (1), 12-31. DOI: 10.1061/(ASCE)1090-0241(2003)129:1(12).
Murali, M. (2011). Characterization of Gulf of Mexico clay using automated triaxial testing. Master's Thesis, Texas A&M University, College Station, TX.
Oikawa, H. (1987). Compression curve of soft soils. Soils and Foundations, Vol. 27(3), 99-104.
Olson, S. M. and Stark, T. D. (2002). Liquefied strength ratio from liquefaction flow failure case histories. Canadian Geotechnical Journal, Vol. 39(3), 629 – 647. DOI:10.1139/t02-001.
Rafalovich, A. and Chaney, R. C. (1990). Correlation between OCR and depth for deep-sea sediments. J. Geotech. Engrg., Vol. 116(11), 1744–1749. DOI: 10.1061/(ASCE)0733-9410(1990)116:11(1744)
Seed, H. B. (1979). Considerations in the earthquake-resistant design of earth and rockfill dams. Géotechnique, Vol. 29(3), 215 – 263. DOI: 10.1680/geot.1979.29.3.215.
Salvador, A. (1991). Origin and development of the Gulf of Mexico Basin. In A. Salvador (ed., The Gulf of Mexico Basin: The geology of North America (Ed., A. Salvador), Geological Society of America, Vol. J., 389 – 444.
Silva, A. J. and Bryant, W. R. (2000). Jumbo Piston Coring in deep water Gulf of Mexico for seabed geohazard and geotechnical investigations. Proceedings of the 10th International Offshore and Polar Engineering Conference, Seattle, U.S., 424–432.
Silva, A., Baxter, C., Bryant, W., Bradshaw, A. and LaRosa, P. (2000). Stress-Strain Behavior and Stress State of Gulf of Mexico Clays in Relation to Slope Processes. Proceedings of the Offshore Technology Conference, Houston, TX. 1–10. DOI:10.4043/12091-MS
Soroush, A., Morgenstern, N.R., Robertson, P.K., and Chan, D. (1996). The earthquake deformation analysis of the Upper San Fernando Dam. Proceedings of the International Symposium on Seismic and Environmental Aspects of Dams Design: Earth, Concrete and Tailing Dams, Santiago, Chile, Vol. 1., 405 – 418.
Stark, T. D. and Mesri, G. (1992). Undrained Shear Strength of Liquefied Sands for Stability Analysis. Journal of Geotechnical Engineering, ASCE, Vol. 118 (11), 1727 – 1747.
Stark, T.D. and Hussain, M. (2013). Drained Shear Strength Correlations for Slope Stability

Analyses. Journal of Geotechnical Engineering, ASCE, Vol. 139(6), 853 – 862.
Terzaghi, K., Peck, R. B., and Mesri, G. (1996). Soil Mechanics in Engineering Practice, 3rd Ed., Wiley, New York.
Thiers, G. R. and Seed, H. B. (1969). Strength and Stress-Strain Characteristics of Clays Subjected to Seismic Loading Conditions. Vibration Effects of Earthquakes on Soils and Foundations, ASTM STP 450, American Society for Testing and Materials, 3 – 56.
Vucetic, M. (1994). Cyclic threshold shear strains in soils. Journal of Geotechnical Engineering, ASCE, Vol. 120(12), 2208–2228. DOI: 10.1061/(ASCE)0733-9410(1994)120:12(2208)
Wang, S. (2011). Postcyclic behavior of low-plasticity silt. Ph.D. dissertation, Missouri University of Science and Technology, Rolla, MO.
Yasuhara, K., Murakami, S., Song, B. W., Yokokawa, S. and Hyde, A. F. L. (2003). Postcyclic degradation of strength and stiffness for low plasticity silt. Journal of Geotechnical and Geoenvironmental Engineering, ASCE, Vol. 129 (8), 756 – 769.